Title

Effect of nitrogen addition on leaf photosynthesis and water use efficiency of the dominant species Leymus chinensis (Trin.) Tzvelev in a semi-arid meadow steppe

Journal

Plant Growth Regulation, 98(1)

ISSN

0167-6903

Authors

Song, Wenzheng

Loik, Michael E

Cui, Haiying

et al.

Publication Date

2022-09-01

DOI

10.1007/s10725-022-00835-8

Plant Growth Regulation (2022) 98:91–102
https://doi.org/10.1007/s10725-022-00835-8

ORIGINAL PAPER

Effect of nitrogen addition on leaf photosynthesis and water use efficiency of the dominant species *Leymus chinensis* (Trin.) Tzvelev in a semi-arid meadow steppe

Wenzheng Song[1] · Michael E. Loik[2] · Haiying Cui[1] · Mingcai Fan[1] · Wei Sun[1]

Received: 30 November 2021 / Accepted: 10 May 2022 / Published online: 6 June 2022

Abstract
Effective utilization of water is the cornerstone of maintaining plant biomass. Water use efficiency (WUE), defined as plant carbon assimilated as biomass per unit of water input, is significantly affected by global change, particularly by nitrogen (N) deposition. Generally, N availability promotes WUE by stimulating photosynthetic. However, the degree to which increased N availability may influence leaf WUE and photosynthesis properties (A, leaf net CO_2 assimilation rate; g_s, stomatal conductance, and E, transpiration rate), especially in salinized-alkalized grasslands, is not studied well. We conducted a randomized block manipulative experiment to evaluate the multilevel N addition (0, 5, 10, 20, 40 g N m^{-2} $year^{-1}$) on leaf photosynthesis properties and leaf WUE of the dominant species (*Leymus chinensis* (Trin.) Tzvelev) in the Songnen meadow steppe from 2016 to 2018. We have three key findings: (1) N availability increased photosynthetic and WUE properties, instantaneous WUE ($W_i = A/E$), intrinsic WUE ($W_g = A/g_s$) and long-term WUE (W_L) inferred from ^{13}C composition, were all showed a non-linear increasing pattern in response to N availability; (2) N application decreased leaf mass per area and increased leaf total N content via enhancing soil inorganic N content, thus increased photosynthetic characteristics (e.g., A, E and g_s), ultimately, promoted W_i and W_g; (3) N application enhanced W_L was attributed to the N-induced improvement in W_i and W_g. Results of the present work are critical to our prediction of how meadow steppe dominated by *L. chinensis* will respond to severe N deposition in the future.

Keywords Nitrogen availability · Photosynthesis rate · Leaf gas exchange · Grassland

Introduction

Excessive demand for irrigation water and climate changes threaten the function of terrestrial ecosystems (Damerau et al. 2019). Thus, effective water utilization is the cornerstone of maintaining plant biomass production. Water use efficiency (WUE) is a composite predictor of plant resistance to water stress, defined as the ratio of plant carbon (C) gain to water use (Condon et al. 2004). Terrestrial ecosystems have experienced ongoing increases in nutrient accumulation since the middle of the 20th century and will continue in the twenty-first century (IPCC 2022). Nitrogen (N), one of the most critical nucleotides and protein components, is related to alterations in plant photosynthetic capacity and WUE under N eutrophication (Liang et al. 2020). It has been demonstrated that increased N availability can enhance plant resistance to drought stress (Cao et al. 2018) and saline-alkaline stress (Fu et al. 2018), increase leaf WUE (Leakey et al. 2019; Liang et al. 2020) and the plant productivity (LeBauer and Treseder 2008; Hao et al. 2020). The above stimulatory effect of N is mainly attributed to the increase in the photosynthetic capacity of leaves (Janssens and Luyssaert 2009). Detailed elucidation of the mechanism by which leaf gas exchange and WUE respond to N could improve our ability to predict the global C dynamics.

Communicated by Zhiqun Huang.

✉ Wei Sun
sunwei@nenu.edu.cn

[1] Institute of Grassland Science, Key Laboratory of Vegetation Ecology of the Ministry of Education, Jilin Songnen Grassland Ecosystem National Observation and Research Station, Northeast Normal University, Changchun, Jilin, People's Republic of China

[2] Department of Environment Studies, University of California, Santa Cruz, CA, USA

Leaf net CO_2 assimilation rate (A), stomatal conductance (g_s), and transpiration rate (E) are significant indicators related to steady-state leaf gas exchange (Flexas et al. 2013). There are two definitions of leaf WUE: one is the intrinsic WUE (W_g), and the other is the transpiration efficiency. The latter can be separated into instantaneous WUE (W_i) and long-term WUE (W_L). For C_3 species, W_g, the ratio of A to g_s, a metric used to characterize the mechanism of carbon and water coupling at the leaf scale (Flexas et al. 2013). Lower g_s restrict A by reducing the stomatal aperture, limiting C assimilation, whereas high g_s promote A at the expense of higher water loss (McAusland et al. 2016). In addition, the N addition exacerbates soil acidification, leading to the leaching of alkaline cations (e.g., Ca^{2+}, K^+ and Mg^{2+}), which are the vital factor that regulates the opening and closing of stomata (Lanning et al. 2019). W_i, the ratio of A to E, reflects stomata control of the balance between the CO_2 uptake for A and the water loss via the transpiration process in leaves (Leakey et al. 2019). The trade-off between A and E is the nexus between ecosystem C and water cycles, underlies global vegetation–climate interactions (Guerrieri et al. 2019). N enrichment can disrupt the stoichiometric balance (Xiao et al. 2017), inevitably leading to changes in photosynthesis and transpiration processes. Estimating C isotope discrimination, W_L provides a time-integrated index reflecting the plant physiology processes (van der Sleen et al. 2017). A meta-analysis showed that the W_L slightly (2.5%) increased with N addition (Liang et al. 2020), while a long-term experiment showed a notable (16.1%) increase with enhancement in N availability (Leonardi et al. 2012). Clarifying how W_L responds to increasing N availability is essential in assessing the sustainability of the grassland ecosystem.

Grasslands are one of the major biomes globally due to their biodiversity and carbon sequestration potential (O'Mara 2012). The Songnen meadow steppe is the most crucial alkali-saline area in northeast China, and the area of saline-alkali land has been increasing due to natural and anthropogenic factors (Yang et al. 2010). It is urgent to explore whether increased N availability raises WUE by affecting C and water processes, or a combination of these two processes and their effects. Using a manipulative experiment with five N addition levels (0, 5, 10, 20, 40 g N m^{-2} $year^{-1}$) in the Songnen meadow steppe, we measured leaf gas exchange indicators (A, E and g_s) and foliar carbon isotope composition ($\delta^{13}C$), leaf mass per area (LMA) and element content of the dominant species *Leymus chinensis* as well as soil physical and chemical properties responded to N enrichment during the growing season (from May to September) for three consecutive years (from 2016 to 2018). We aimed to explore how increased N availability improves plant leaf-level gas exchange and WUE. We have three hypotheses: (1) N addition would promote photosynthetic properties (A, E and g_s) and WUE (W_i, W_g and W_L); (2) N addition would enhance CO_2 assimilation via increasing stomatal opening (expressed as g_s), with an acute effect on A than g_s; and (3) N addition would increase W_L by regulating plant physiological and morphological adaptation.

Materials and methods

Study site

A semi-arid meadow steppe located in the Jilin Songnen Grassland Ecosystem National Observation and Research Station (44°45′N, 123°45′E; western Jilin Province, northeast China) was selected to conduct this experiment. The climate is a monsoon climate of medium latitudes (Chai et al. 2022; Yang et al. 2020). The average annual temperature and precipitation (1953–2017) were 5.6 °C and 445 mm, respectively. The average (1953–2017) growing season (from May to September) precipitation was 383.4 mm. Soil pH ranges from 7.5 to 9.0, and soil total N content was 1.01 g kg^{-1} (Meng et al. 2021). The dominated species was the C_3 rhizomatous grass *Leymus chinensis*; other common species include but are not limited to the graminoids *Phragmites australis*, *Calamagrostis epigeios* and *Carex duriuscula*; the forbs *Potentilla flagellaris* and *Kalimeris integrifolia*; and the legumes *Lespedeza davurica* and *Medicago ruthenica* (Cui et al. 2021; Wang et al. 2019).

Experimental design

Two ha (100 m × 200 m) area of the grassland (historically used for light grazing and hay production) was fenced to exclude disturbances in 2010. Previous studies have reported experimental design and fertilizer treatments (Cui et al. 2021). In April 2015, we established eight blocks (34 m × 32 m) with similar vegetation conditions. In each block, we set up 18 plots (5 m × 10 m) and separated the adjacent plots by a 1 m wide buffer strip. For the present study, five plots (in each block) were used and randomly assigned one of the following N addition rates (0, 5, 10, 20 and 40 g N m^{-2} $year^{-1}$), and the N fertilizer was applied as a mixture of NH_4NO_3 and Urea at a ratio of 7:3 with eight replicates. To assure that the experimental plants were only affected by N (Tilman 1987), we added other elements including P (10 g P m^{-2} $year^{-1}$; $(H_2PO_4)_2{\cdot}H_2O$); Fe (190 μg m^{-2} $year^{-1}$; $FeSO_4{\cdot}7H_2O$); Mn (160 μg m^{-2} $year^{-1}$; $MnSO_4{\cdot}H_2O$); Zn (190 μg m^{-2} $year^{-1}$; $ZnSO_4{\cdot}7H_2O$), Cu (15 μg m^{-2} $year^{-1}$; $CuSO_4{\cdot}5H_2O$); B (31 μg m^{-2} $year^{-1}$; $Na_2B_4O_7{\cdot}10H_2O$); Mo (1.4 μg m^{-2} $year^{-1}$; $Na_2MoO_4{\cdot}2H_2O$) for all treatments (Bai et al. 2010). Fertilization treatments have been applied once a month during the growing season from May to September. The applied fertilizers were dissolved in 5 L deionized water

and sprayed evenly on each plot with a sprayer. Blank plots (0 g N m^{-2} $year^{-1}$) received equal amounts of deionized water.

Environmental factors

An automatic weather station (HOBO U30-NRC; Onset Computer Corporation, Bourne, MA, USA) was installed at the experimental site to collect the daily cumulative precipitation and daily mean air temperature data. The soil moisture (SM) and soil temperature (ST) at 10 cm depth were measured concurrently with leaf gas exchange measurement (see below). ST was measured using a temperature probe (6000-09TC) coupled to an infrared gas analyzer (Li-6400, Li-COR Inc., Lincoln, NE, USA). SM was measured using the drying method (drying 10 g of fresh soil to a constant weight at 105 °C). Soil pH was analyzed (air-dried soil:deionized water = 1:5) with a pH meter (PHS-3E INESA Scientific Instrument Co., Ltd, Shanghai, P.R. China).

Leaf gas exchange measurement

An open infrared portable photosynthesis system (LI-6400, Li-Cor Inc., Lincoln, NE, USA), connected to a standard 20 × 30 mm chamber with a LED light source (6400-02B) and a CO_2-mixing device controlling the level of reference CO_2, was used to measure leaf gas exchange parameters (A, E and g_s). The measurement was conducted between 8:00 and 11:00 AM on a cloud-free day (Niu et al. 2011) from May to July, and the frequency was once per month. Specifically, photosynthesis measurements were conducted on 15 May, 18 June, 20 July in 2016, 20 May, 15 June, 17 July in 2017, and 25 May, 22 June, and 24 July in 2018, respectively. Five healthy upper-most fully expanded leaves (the 3rd leaf from the top) of the dominant species *L. chinensis* were randomly selected on each plot for photosynthesis measurements. After the gas analyzers were warmed up and calibrated, the following protocols were conducted for leaf gas exchange measurements. Expressly, inside the leaf chamber, we set the PPFD at 1500 μmol m^{-2} s^{-1}, the CO_2 concentration at 400 ppm, the flow rate at 500 μmol s^{-1}, block temperature at 25 °C, and relative humidity adjusted to 45–60%. One matching operation was performed for each leaf. Leaves were acclimated to the chamber condition for at least 3 min until A and g_s stabilized (coefficient of variation (CV) < 1%). There were eight replicate measurements per treatment.

LMA measurement

Five leaves of the dominant species *L. chinensis* performed the gas exchange measurements were collected to calculate leaf mass per area (LMA). After scanning, the leaf area was calculated using Image J 1.47d (National Institute of Health, Washington D. C., USA). Then, plant materials were oven-dried at 65 °C to a constant weight. LMA was calculated as the mass values of the area (Edwards et al. 2014). Then, the dry leaf materials were crushed using a ball mill (MM 400 Retsch, Hanau, Germany) and sieved through a mesh (100 mm mesh) to analyze elemental contents.

Soil sample collection

We selected three soil cores (0–10 cm in-depth, 3 cm in diameter) in each quadrat used for plant biomass harvesting and mixed them into a composite sample. Then, the coarser roots and stones were removed and sieved through a mesh (2 mm mesh). The soil sample was then divided into two parts: one for measuring soil inorganic N content (SIN, the sum of soil nitrate and ammonium N content) and the other part, which was naturally air-dried and sieved through a mesh (100 mm mesh) for measuring soil nutrient content.

Foliar and soil nutrient contents

We analyzed the leaves and soil's total N content (TN) with an elemental analyzer (Vario EL III, Elementar Inc., Hanau, Germany). Total phosphorus content (TP) of the leaves was determined by digesting foliar samples with H_2SO_4 and $HClO_4$ at 380 °C for 3 h, then measuring colorimetrically at a wavelength of 700 nm (Olsen et al. 1954) using a UV spectrophotometer (UV-5500, Shanghai Yuan-Analysis Instrument CO., LTD., Shanghai, P.R. China). SIN was determined by extracting soil samples with 2 M KCl and analyzed using a continuous flow analyzer (Futura Segmented Flow Analysis, Alliance-AMS., France). The soil was extracted with 0.5 M $NaHCO_3$ (pH = 8.5) for 1 h at 180 rpm and analyzed colorimetrically at a wavelength of 880 nm using a UV spectrophotometer to test the soil available phosphorus (AP).

Stable isotope analysis

In August of each experimental year, we collected the third fully unfolded and mature leaf from the top of the dominated species *L. chinensis* to evaluate W_L. An isotope ratio mass spectrometry (IsoPrime100; Isoprime Ltd., Stockport, UK) was selected to analyze leaf stable carbon isotope composition ($\delta^{13}C$). $\delta^{13}C$ was calculated as Eq. 1:

$$\delta^{13}C = 1000 \times \left(\frac{R_{sample}}{R_{standard}} - 1 \right) \quad (1)$$

where R_{sample} and $R_{standard}$ denote the molar fraction of the $^{13}C/^{12}C$ ratio of the sample and the Pee Dee Belemnite international standard (Lavergne et al. 2019), respectively. In addition, plants prefer to use ^{12}C than ^{13}C during

photosynthesis, which resulted in carbon isotopic discrimination against ^{13}C ($\Delta^{13}C$), and the $\Delta^{13}C$ was defined as Eq. 2 (Farquhar and Cernusak 2012; Lavergne et al. 2019),

$$\Delta^{13}C = \frac{\delta^{13}C_a - \delta^{13}C_p}{1+\frac{\delta^{13}C_p}{1000}} \quad (2)$$

where $\delta^{13}C_a$ and $\delta^{13}C_p$ denote the $\delta^{13}C$ values of atmospheric CO_2 and plant tissue, respectively.

The previous study has demonstrated a relationship between $\delta^{13}C_a$ and calendar year (t) as Eq. 3 (Feng 1999)

$$\delta^{13}C_a = -6.429 - 0.006e^{0.0217(t-1740)} \quad (3)$$

For C_3 plants, there is a linear relationship between the $\Delta^{13}C$ and c_i/c_a during CO_2 fixation (Lavergne et al. 2019):

$$\Delta^{13}C = a + (b-a)\frac{c_i}{c_a} \quad (4)$$

where a (4.4‰) referred to the enrichment during CO_2 diffusion and b (27‰) was the fractionation by the ribulose-1, 5-biphosphate carboxylase oxygenase (Rubisco) against $^{13}CO_2$ (Farquhar et al. 1982). A linear relationship between c_a and the calendar year (t) as Eq. 5 (Feng 1999),

$$c_a = 277.78 + 1.35e^{0.0157(t-1740)} \quad (5)$$

Besides, the molar diffusivity of CO_2 is 1.6 times that of water (Guerrieri et al. 2019). Therefore, we can derive the Eq. 6:

$$\frac{A}{g_s} = \frac{(c_a - c_i)}{1.6} \quad (6)$$

By combining Eq. 2, Eq. 4, and Eq. 6, we can derive the W_L as the Eq. 7:

$$W_L = \frac{c_a(b-\Delta^{13}C)}{1.6(b-a)} \quad (7)$$

Statistical analyses

One-way ANOVA with post hoc Tukey's HSD test was used to test the main effects of N addition on soil (e.g., ST, SM, pH, SIN and AP), plant (e.g., LMA, TN, TP, C:N ratio and N:P ratio), leaf carbon exchange (e.g., A, E and g_s) and leaf scale WUE (e.g., W_i, W_g and W_L). Regression models were conducted to establish the relationship between soil and plant characteristics with different levels of N addition. The relative changes of X (e.g., photosynthetic characteristics, WUE, plant and soil parameters) across three years were calculated as Eq. 8:

$$\text{Relative changes of X} = \frac{X_M - X_0}{X_0} \times 100\% \quad (8)$$

where X_M and X_0 denote the X values in M g N m^{-2} $year^{-1}$ and 0 g N m^{-2} $year^{-1}$, respectively. All statistical analysis was performed with SPSS software (SPSS 22.0 for windows, IBM-SPSS Inc., Chicago, IL, USA).

We selected Structural Equation Modeling (SEM) to identify direct and indirect responses of photosynthesis and WUE indicators to N availability (Grace et al. 2010). We developed an *a priori* model based on previous knowledge, which assumed that N availability alters SIN, further affects plant morphology (LMA) and photosynthesis-related traits (e.g., TN, A, E and g_s) (Ruiz et al. 2008). We assessed the model goodness-of-fit, including the chi-square statistic ($0 \le \chi^2/df \le 2$, where $P > 0.05$ was considered adequate), root mean square error of approximation ($0 \le RMSEA \le 0.05$), and standardized root mean square residual ($0 \le SRMR \le 0.05$) (Delgado-Baquerizo et al. 2016). A Pseudo-R^2 was calculated for response variables (Lefcheck 2016). SEM models and all graphics were conducted by R v.3.6.3 software (R Development Core Team 2020).

Results

Precipitation and air temperature during the growing season

The highest air temperature occurred in the middle of the growing season of all experimental years (Fig. 1). The growing season precipitation displayed differences in amount and distribution across the experimental years (Fig. 1). Compared to average growing season precipitation (1953–2017, 383.4 mm) of this region, 2016 (412.0 mm; + 7.5%) and 2017 (415.4 mm; + 8.3%) were slightly wet years, whereas 2018 (315.0 mm; − 17.8%) was a relatively dry year (Fig. 1D). The coefficient of variation (CV) of the monthly precipitation during the growing season (from May to September) was 71.42%, 147.73% and 86.70% in 2016, 2017 and 2018.

Responses of soil and plant physicochemical indicators to N addition

ST showed a non-linear decrease with increasing N concentration (Fig. 2A). However, N addition had no pronounced effects on SM (Fig. 2B and Table S1). The pH had a linear decrease (Fig. 2C) even though there were no significant differences in 2016 and 2017 (Table S1). However, ongoing treatments significantly decreased soil pH at the N addition rate of 20 g N m^{-2} $year^{-1}$ in 2018 (Table S1). In addition,

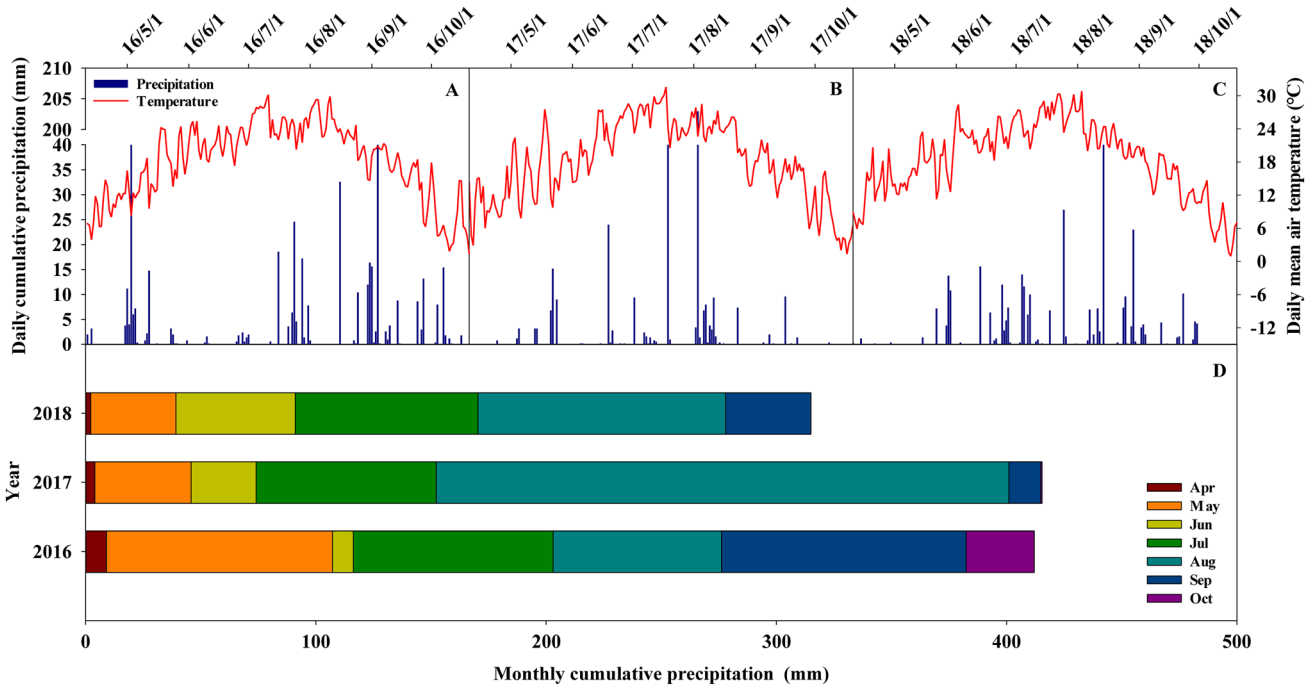

Fig. 1 Seasonal patterns of daily precipitation (blue bars, mm), daily mean air temperature (red lines, °C) in 2016 (**A**), 2017 (**B**) and 2018 (**C**), and growing season accumulative precipitation in 2016, 2017 and 2018 (**D**). (Color figure online)

SIN and AP showed increasing and decreasing non-linear trends with increasing N concentration, respectively (Fig. 2D). LMA decreased non-linearly with the increasing N concentration (Fig. 2F). The TN of the dominant species *L. chinensis* increased significantly with N additions (Fig. 2G and Table S1); however, that of TP had the opposite direction (Fig. 2H and Table S1). Changes in TN and TP further led to a significant increase in the leaf N:P ratios (Fig. 2J). The leaf C: N ratio increased significantly with N additions (Fig. 2I and Table S1).

Responses of photosynthetic properties to N addition

N application significantly affected the photosynthetic properties (A, g_s and E) across all experimental years. More specifically, both A (Fig. 3A, B) and g_s (Fig. 3C, D) showed an increasing trend with increasing N availability. However, the response pattern of E showed first a decreasing and then an increasing trend (Fig. 3E, F). The results for each sampling year and the average values showed no significant differences among different N addition rates. The relative changes of A showed an increasing trend with increasing N availability. A significant difference appeared when the N concentration reached 40 g N m^{-2} $year^{-1}$ (Fig. 3G). At the same time, g_s showed a non-significant increasing trend (Fig. 3H). The relative changes of E were similar to that of average values, but no significant differences among different N addition rates (Fig. 3I).

Responses of WUE to N addition

N availability increased WUE across all experimental years except for W_g, which firstly increased and then decreased in 2018 (Fig. 4C). In 2017, W_g and W_L showed significant differences at 40 g N m^{-2} $year^{-1}$ (N_{40}) and 20 g N m^{-2} $year^{-1}$ (N_{20}) treatments, respectively (Fig. 4C, E). However, the other treatment years showed an increasing trend but no significant differences among different treatments (Fig. 4A, C, E). The average results showed a parabolic relationship (with a downward opening) between WUE and N addition rate (Fig. 4B, D, F). The saturation response of W_i and W_L appeared at the N_{20} and N_{40} treatments, respectively (Fig. 4B, F). There was a positive correlation between N availability and the relative change of WUE, but no significant effect across treatments (Fig. 4G, H), except for W_L, which had a significant increase at the N_{40} (Fig. 4I).

Abiotic and biotic factors influencing leaf photosynthetic properties and WUE

The results of SEM model analysis revealed that N application enhanced SIN, leaf TN, decreased LMA directly, and decreased LMA indirectly by promoting SIN. SIN and TN increased A, E, and W_i. A was directly affected by decreased

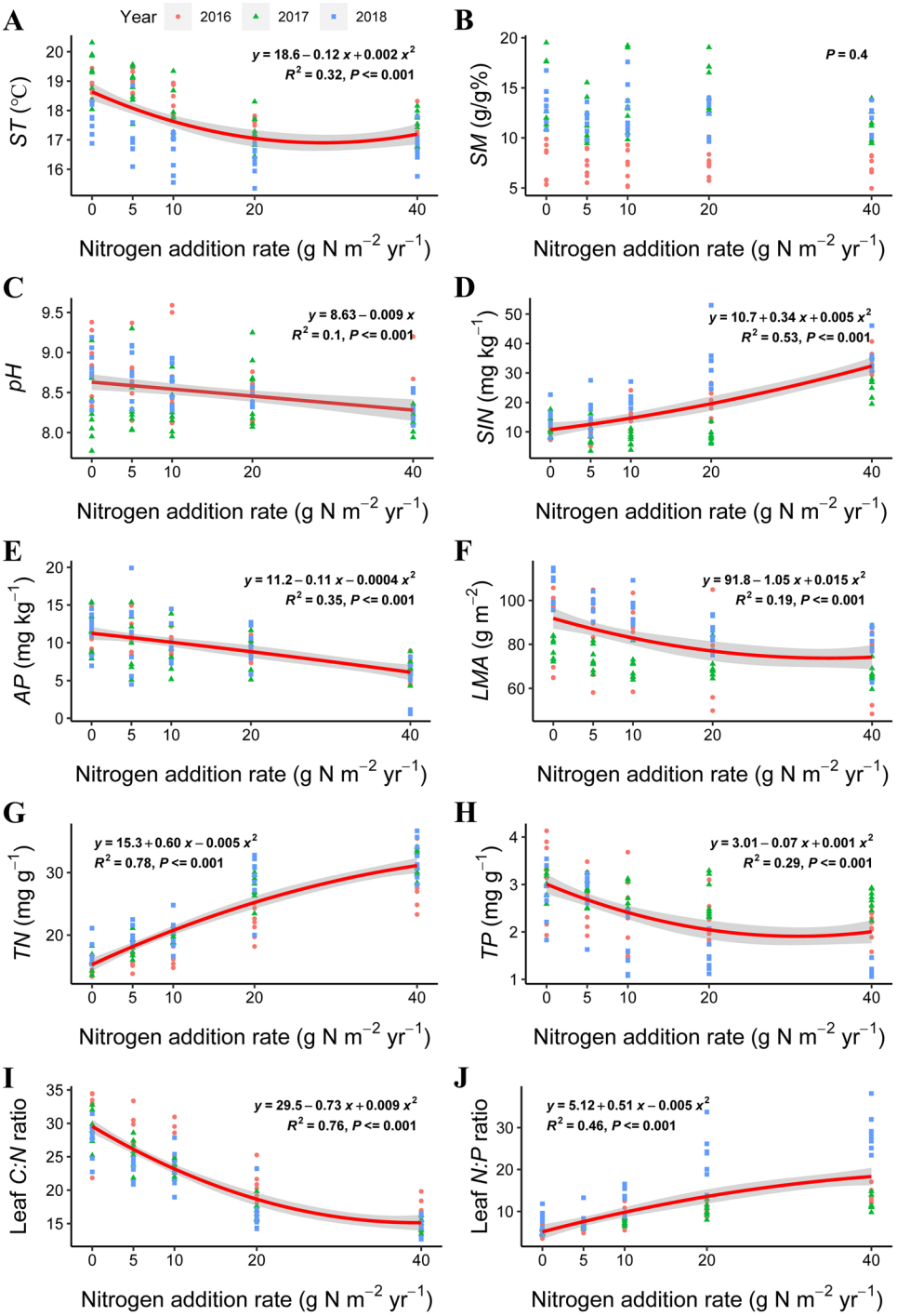

Fig. 2 Responses of soil (surface layer; 10 cm) and plant variables to N addition rate (n = 8). *ST* soil temperature, *SM* soil moisture, *pH* soil pH, *SIN* soil inorganic N content, *AP* soil available phosphorous content, *LMA* leaf mass per unit area, *TN* plant total N content, *TP* plant total phosphorous content, *C:N ratio* the ratio of leaf total carbon content to TN, *N:P ratio* the ratio of TN to TP

LMA. TN and SIN impacted W_i indirectly combined with A and E. The direct and indirect pathways explained 27%, 17%, and 19% of the total variance in A, E, and W_i, respectively (Fig. 5A). For W_g, A was affected by SIN, TN, and LMA, but g_s was not affected by TN. TN and SIN impacted W_g in combination with A and g_s. Eventually, the direct and indirect pathways explained 29%, 16%, and 13% of the total variation in A, g_s, and W_g, respectively (Fig. 5B). TN and SIN promoted W_i, W_g, and W_L. W_i and W_g impacted W_L combined with LMA. Ultimately, the direct and indirect pathways could explain 19%, 15%, and 14% of the total variation in W_i, W_g and W_L (Fig. 5C).

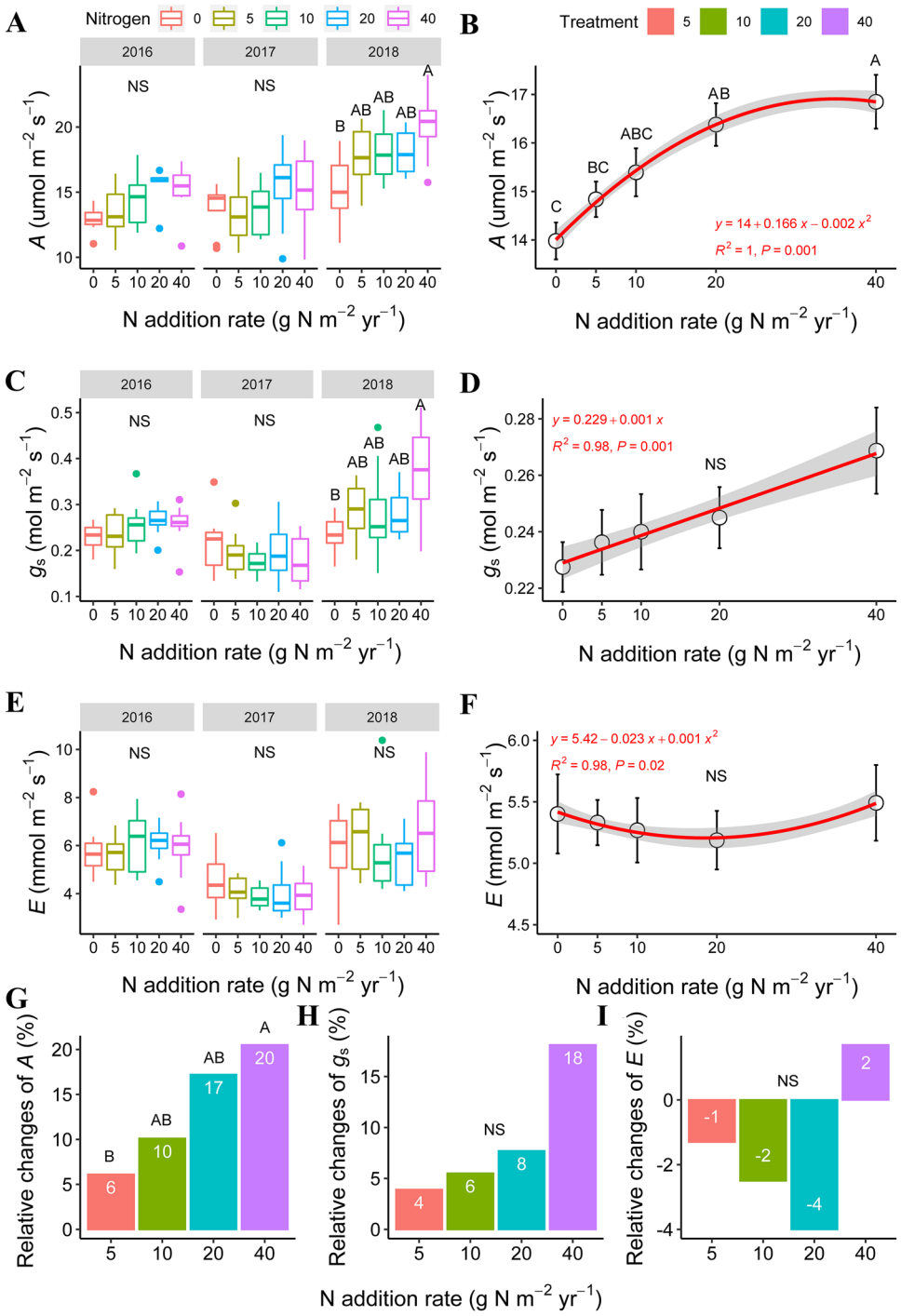

Fig. 3 Effects of N addition on leaf net CO_2 assimilation rate (A, μmol CO_2 m^{-2} s^{-1}), stomatal conductance (g_s, mol H_2O m^{-2} s^{-1}) and transpiration rate (E, mmol H_2O m^{-2} s^{-1}) in each year (A, **A**; g_s, **C**; E, **E**), mean results across all years (A, **B**; g_s, **D**; E, **F**) and mean N-induced relative changes across all years (A, **G**; g_s, **H**; E, **I**). Different letters present a significant difference ($P < 0.05$) among different N addition rates. Error bars denote standard errors ($n = 8$)

Discussion

Environmental factors influence photosynthetic properties

N availability promoted plant growth and enhanced canopy cover at the community scale (Liang et al. 2020), decreasing the ST. Previous studies have demonstrated that the lower ST could reduce the N mineralization rate (Deng et al. 2018), which further induces a deficit of available N resources in the soil for maintaining plant photosynthetic physiological processes, ultimately generating a non-linear response between photosynthetic physiological indicators and N concentrations.

Water stress mainly affects A due to decreased g_s (McAusland et al. 2016). In this study, A and g_s varied significantly over the three experimental years, mainly attributed to the seasonal distribution of precipitation,

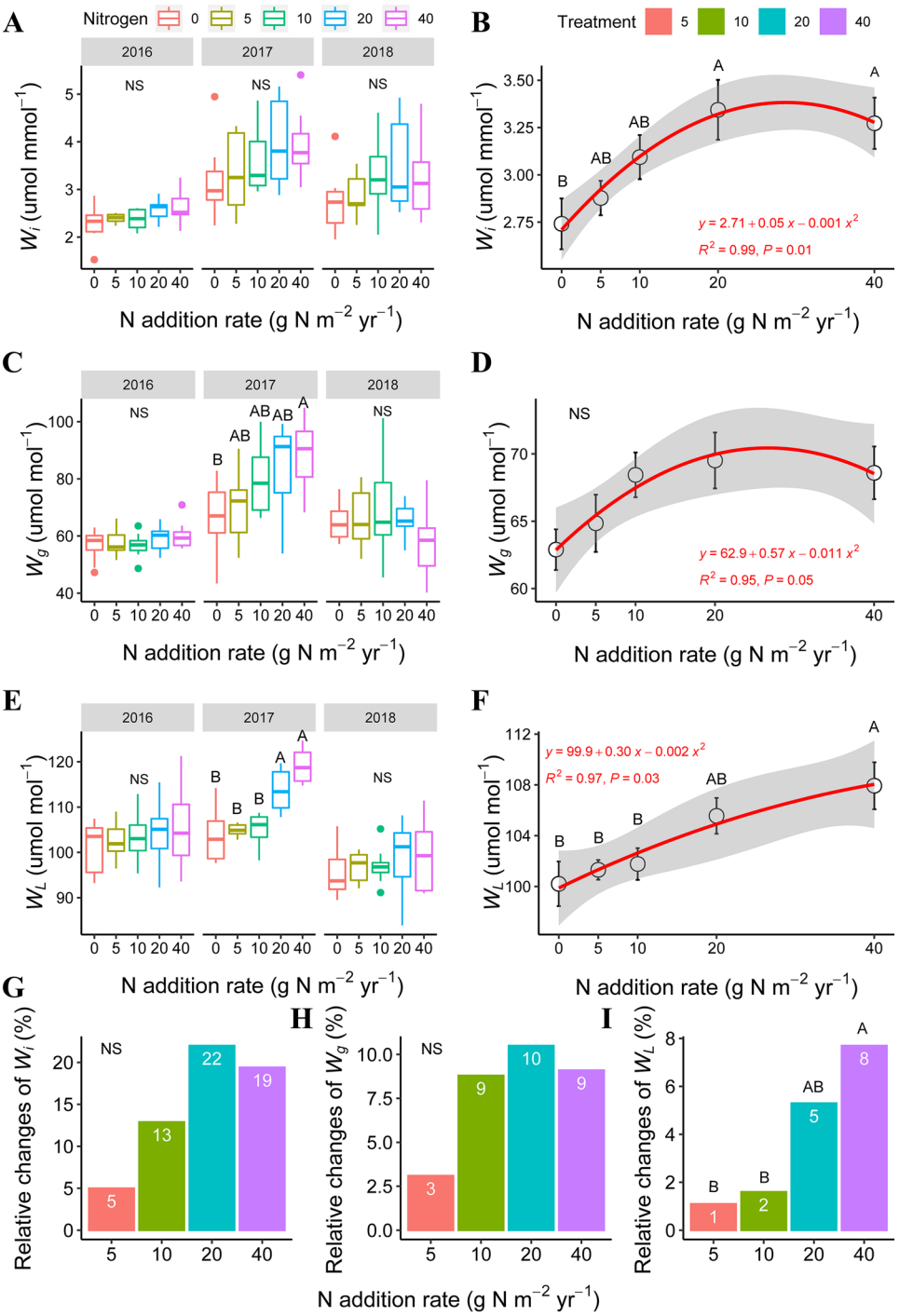

Fig. 4 Effects of N addition on instantaneous water use efficiency (W_i, μmol CO_2 mmol H_2O^{-1}), intrinsic water use efficiency (W_g, μmol CO_2 mol H_2O^{-1}) and long-term water use efficiency (W_g, μmol CO_2 mol H_2O^{-1}) in each year (W_i, **A**; W_g, **C**; W_L, **E**), mean results across all years (W_i, **B**; W_g, **D**; W_L, **F**) and mean N-induced relative changes across all years (W_i, **G**; W_g, **H**; W_L, **I**). Different letters present a significant difference ($P < 0.05$) among different N addition rates. Error bars denote standard errors (n = 8)

consistent with the findings that A and g_s of the dominant species (*L. chinensis*) decreased significantly with lower water availability (Li et al. 2019). In this study, measurements occurred from May to July, and the rainfall during the sampling period corresponded to 49.3% (203.1 mm; 2016), 36.6% (152.0 mm; 2017), and 54% (170.2 mm; 2018) of the annual growing season rainfall (383.4 mm; 1953–2017). Compared to 2016 and 2018, 2017 was a relatively dry year. Therefore, both A and g_s decreased. However, in 2018, the rainfall was more evenly distributed, which likely favored the early growth of the plants and thus maintained high A and g_s. In other words, N availability significantly reduced A and g_s in the dry year (2017) but showed the opposite response patterns in the wetter years (2016 and 2018). The above results suggested that plants tend to be more sensitive to drought under N availability (Shi et al. 2018) due to their high water requirement (Gessler et al. 2017; Meng et al. 2021).

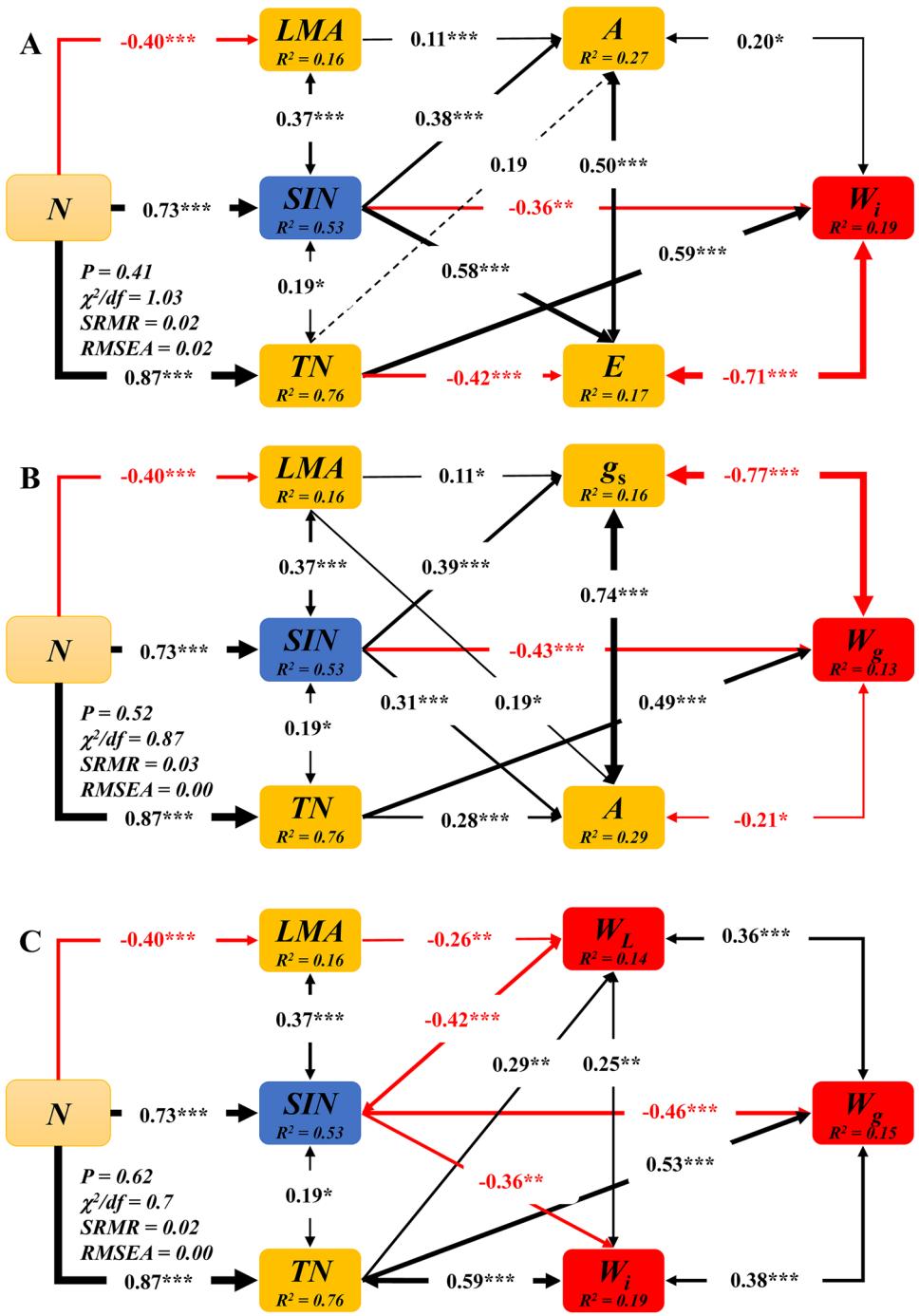

Fig. 5 Structural equation modeling (SEM) of N effects on water use efficiency. The black and red solid arrows indicate positive and negative relationships, respectively. Values at arrows represent standardized path coefficients, and the thickness of the arrows is proportional to the strength of the relationship. R^2 values in the variable box indicate the proportion of variation explained by all relevant variables. *N* nitrogen addition, *LMA* leaf mass per unit area, *SIN* soil inorganic N content, *TN* plant total N content, *A* leaf net CO_2 assimilation rate, g_s stomatal conductance, and *E* transpiration rate, W_i instantaneous WUE, W_g instantaneous WUE and W_L long-term WUE. *, ** and *** indicates significant differences at $P<0.05$, $P<0.01$, $P<0.001$, respectively

The pH closely relates to plants' productivity (Tian et al. 2016). We confirmed that the soil pH decreased as N availability increased, which was in line with a study in a tropical forest ecosystem (Mao et al. 2018). Undeniably, N enrichment will lead to soil acidification, thus threatening plant growth (Stevens et al. 2015). However, soil pH in our study showed a linear decreased tendency, which inevitably has a positive impact on the photosynthetic to some extent due to the original high pH of the present experimental area (Wang et al. 2020). It provides an explanatory pathway for the non-linear results between photosynthetic indicators and N availability.

N availability promotes plant C uptake by stimulating the photosynthetic capacity of leaves (Janssens and Luyssaert 2009). This study found that N application affected *A*, and had interrelated effects on g_s and *E*. We found that the *A* in N_{10} treatment was increased by 10% than that in N_0, which is close to the results of a recent meta-analysis (including 320 terrestrial plant species from different functional types), which found that N addition at 10 g N m^{-2} $year^{-1}$ increased

A by 12.6% (Liang et al. 2020), suggests that C assimilation will be enhanced with increasing N availability. We found a continuous increase in g_s with increasing N availability, inconsistent with a previous study that found N addition will exacerbate soil acidification. The decreased pH may lead to the leaching of alkaline cations (e.g., Ca^{2+}, K^+ and Mg^{2+}), which are vital factors related to stomata opening and closing (Lanning et al. 2019). That result was probably attributed to the high initial pH in this grassland. A degree of reduction in soil pH as N availability increases may benefit the plant's growth.

The stability of elemental stoichiometry is essential for plant growth (Xiao et al. 2017; Peng et al. 2017). A study reported that long-term N addition enhanced overall photosynthesis in terrestrial systems by 18.4% via increasing TN (Liang et al. 2020). Our study found that the TN of *L. chinensis* increased significantly with N gradients, similar to a previous meta-analysis that showed a 19.6% increase in TN at 10 g N m^{-2} $year^{-1}$ (Ostertag and DiManno 2016). Plant N:P ratio has a remarkable impact on revealing C dynamics in increased N availability. For instance, plant biomass was mainly N-limited when the N:P ratio was < 14. However, resource limitations were shifted from N-limited to P-limited once N:P ratio was > 16 (Peng et al. 2017). Our result confirmed that photosynthetic characteristics did not increase with a sustained increase in N availability, and the N:P ratio would adequately be a validated pathway. In this study, we found that the N:P ratio of the dominant species (*L. chinensis*) ranged from 4.9 ± 0.5 (Table S1, N_0 in 2016) to 28.8 ± 1.6 (Table S1, N_{40} in 2018). Therefore, ongoing N addition may lead to an imbalance of leaf stoichiometry, resulting in limiting resources shifted from N to phosphorus.

Responses of leaf water use efficiency to N addition

We found no significant difference in WUE with a continuous increase in N concentration, similar to a recent meta-analysis, which reported no significant change in W_i with N availability (Liang et al. 2020). Compared to W_g, however, W_i had a more robust response to N availability (Fig. 4G, H). The main reason for this phenomenon was that N-induced relative change in g_s was more significant than that in *E* (Fig. 3H, I). The results of W_L calculated by the isotope technique increased significantly with increasing N availability than that of W_i and W_g, which would be attributed to the fact that the isotopic technique is a comprehensive reflection of the changes in the external environment (e.g., climatic conditions, light, nutrients, water) experienced throughout its lifetime (van der Sleen et al. 2017). Our findings were similar to a recent meta-analysis that found W_L shows a slight increase (2.5%) with the addition of N (Liang et al. 2020). And that was lower than a previous study which found a significantly increasing trend (16.1%) of W_L with a long-term (from 1850 to 2000) N deposition (Leonardi et al. 2012). Therefore, both the treatment time and the cumulative effect of N may play equally important roles in assessing the plant's response to future N deposition (Yu et al. 2019). SEM results suggested that the following mechanisms can explain the response of leaf WUE to N availability. N addition enhances soil SIN and then affects the response of leaf morphology (e.g., LMA) and stoichiometry (e.g., TN), thus increasing photosynthetic characteristics (e.g., *A*, *E* and g_s). N-enhanced leaf W_L was attributed to the cumulative N-induced increase in W_i and W_g within a given growth cycle.

Conclusions

In summary, there were three key findings: (a) N addition significantly increased *A* and g_s in the dry year but not in the wetter years, and the increase in *A* was more extensive than that of g_s could be used to interpret the positive correlation between W_g and N availability; (b) leaf WUE (e.g., W_i, W_g and W_L) were all showed a non-linear enhancement with increasing available N content, and the increase in N availability leads to a break in stoichiometry balance and further induced resource limitation shift from N to other resources; (c) N application decreased LMA and increased TN via enhancing SIN, which enhanced photosynthetic characteristics (e.g., *A*, *E* and g_s), thus promoted W_i and W_g. Additionally, enhanced W_L under N enrichment was attributed to the N-induced improvement in W_i and W_g.

Supplementary information The online version contains supplementary material available at https://doi.org/10.1007/s10725-022-00835-8.

Acknowledgements We thank Jing Gao, Xiaoli Ling, and Keying Wang for their help with field and laboratory work.

Author contributions WZS and WS designed the experiment; WZS, HYC, and MCF conducted the field and laboratory experiments; WZS analyzed the data and wrote the manuscript with great assistance from MEL and WS. All authors provided input to the drafting and final version of the manuscript.

Funding This study was funded by the National Natural Science Foundation of China (No. 31570470, 31870456) and the Program of Introducing Talents of Discipline to Universities (No. B16011). W.Z.S. acknowledges scholarship support from China Scholarship Council (CSC, No. 202106620024).

Data availability The datasets analyzed during the current study are available from the corresponding author on reasonable request.

Declarations

Conflict of interest The authors declare that they have no known competing financial interests or personal relationships that could have appeared to influence the work reported in this paper.

References

Bai Y, Wu J, Clark CM, Naeemz S, Pan Q, Huang J, Hang L, Han X (2010) Tradeoffs and thresholds in the effects of nitrogen addition on biodiversity and ecosystem functioning: evidence from inner Mongolia Grasslands. Glob Change Biol 16(1):358–372. https://doi.org/10.1111/j.1365-2486.2009.01950.x

Cao X, Zhu C, Zhong C, Hussain S, Zhu L, Wu L, Jin Q (2018) Mixed-nitrogen nutrition-mediated enhancement of drought tolerance of rice seedlings associated with photosynthesis, hormone balance and carbohydrate partitioning. Plant Growth Regul 84(3):451–465. doi:https://doi.org/10.1007/s10725-017-0352-6

Chai H, Li J, Ochoa-Hueso R, Yang X, Li J, Meng B, Song W, Zhong X, Ma J, Sun W (2022) Different drivers of soil C accumulation in aggregates in response to altered precipitation in a semiarid grassland. Sci Tot Environ 830:154760. doi:https://doi.org/10.1016/j.scitotenv.2022.154760

Condon AG, Richards RA, Rebetzke GJ, Farquhar GD (2004) Breeding for high water-use efficiency. J Exp Bot 55(407):2447–2460. doi:https://doi.org/10.1093/jxb/erh277

Cui H, Sun W, Delgado-Baquerizo M, Song W, Ma JY, Wang K, Ling X (2021) Cascading effects of N fertilization activate biologically driven mechanisms promoting P availability in a semi-arid grassland ecosystem. Funct Ecol 35(4):1001–1011. doi:https://doi.org/10.1111/1365-2435.13773

Damerau K, Waha K, Herrero M (2019) The impact of nutrient-rich food choices on agricultural water-use efficiency. Nat Sustain 2(3):233–241. doi:https://doi.org/10.1038/s41893-019-0242-1

Delgado-Baquerizo M, Maestre FT, Reich PB, Jeffries TC, Gaitan JJ, Encinar D, Berdugo M, Campbell CD, Singh BK (2016) Microbial diversity drives multifunctionality in terrestrial ecosystems. Nat Commun 7(1):1–8. doi:https://doi.org/10.1038/ncomms10541

Deng M, Liu L, Jiang L, Liu W, Wang X, Li S, Yang S, Wang B (2018) Ecosystem scale trade-off in nitrogen acquisition pathways. Nat Ecol Evol 2(11):1724–1734. doi:https://doi.org/10.1038/s41559-018-0677-1

Edwards EJ, Chatelet DS, Sack L, Donoghue MJ (2014) Leaf life span and the leaf economic spectrum in the context of whole plant architecture. J Ecol 102(2):328–336. doi:https://doi.org/10.1111/1365-2745.12209

Farquhar GD, Cernusak LA (2012) Ternary effects on the gas exchange of isotopologues of carbon dioxide. Plant Cell Environ 35(7):1221–1231. doi:https://doi.org/10.1111/j.1365-3040.2012.02484.x

Farquhar GD, O'Leary MH, Berry JA (1982) On the relationship between carbon isotope discrimination and the intercellular carbon dioxide concentration in leaves. Australian J Plant Physiol 9(2):121–137. doi:https://doi.org/10.1071/PP9820121

Feng X (1999) Trends in intrinsic water-use efficiency of natural trees for the past 100–200 years: a response to atmospheric CO_2 concentration. Geochim Cosmochim Acta 63(13–14):1891–1903. doi:https://doi.org/10.1016/S0016-7037(99)00088-5

Flexas J, Niinemets U, Gallé A, Barbour MM, Centritto M, Diaz-Espejo A, Douthe C, Galmés J, Ribas-Carbo M, Rodriguez PL, Rosselló F, Soolanayakanahally R, Tomas M, Wright IJ, Farquhar GD, Medrano H (2013) Diffusional conductances to CO_2 as a target for increasing photosynthesis and photosynthetic water-use efficiency. Photosynth Res 117(1–3):45–59. doi:https://doi.org/10.1007/s11120-013-9844-z

Fu J, Wang YF, Liu ZH, Li ZT, Yang KJ (2018) Trichoderma asperellum alleviates the effects of saline–alkaline stress on maize seedlings via the regulation of photosynthesis and nitrogen metabolism. Plant Growth Regul 85(3):363–374. doi:https://doi.org/10.1007/s10725-018-0386-4

Gessler A, Schaub M, McDowell NG (2017) The role of nutrients in drought-induced tree mortality and recovery. New Phytol 214(2):513–520. doi:https://doi.org/10.1111/nph.14340

Grace JB, Michael Anderson T, Han O, Scheiner SM (2010) On the specification of structural equation models for ecological systems. Ecol Monogr 80(1):67–87. doi:https://doi.org/10.1890/09-0464.1

Guerrieri R, Belmecheri S, Ollinger SV, Asbjornsen H, Jennings K, Xiao J, Stocker BD, Martin M, Hollinger DY, Bracho-Garrillo R, Clark K, Dore S, Kolb T, William Munger J, Novick K, Richardson AD (2019) Disentangling the role of photosynthesis and stomatal conductance on rising forest water-use efficiency. Proc Natl Acad Sci USA 116(34):16909–16914. doi:https://doi.org/10.1073/pnas.1905912116

Hao X, Jia J, Mi J, Yang S, Khattak AM, Zheng L, Gao W, Wang M (2020) An optimization model of light intensity and nitrogen concentration coupled with yield and quality. Plant Growth Regul 92(2):319–331. doi:https://doi.org/10.1007/s10725-020-00641-0

IPCC (2022) Climate Change 2022: Mitigation of Climate Change. Contribution of Working Group III to the Sixth Assessment Report of the Intergovernmental Panel on Climate Change. Cambridge University Press, Cambridge, United Kingdom and New York, NY, USA. doi:https://doi.org/10.1017/9781009157926

Janssens IA, Luyssaert S (2009) Carbon cycle: Nitrogen's carbon bonus. Nat Geosci 2(5):318–319. doi:https://doi.org/10.1038/ngeo505

Lanning M, Wang L, Scanlon TM, Vadeboncoeur MA, Adams MB, Epstein HE, Druckenbrod D (2019) Intensified vegetation water use under acid deposition. Sci Adv 5(7):eaav5168. doi:https://doi.org/10.1126/sciadv.aav5168

Lavergne A, Graven H, De Kauwe MG, Keenan TF, Medlyn BE, Prentice IC (2019) Observed and modelled historical trends in the water-use efficiency of plants and ecosystems. Glob Change Biol 25(7):2242–2257. doi:https://doi.org/10.1111/gcb.14634

Leakey ADB, Ferguson JN, Pignon CP, Wu A, Jin Z, Hammer GL, Lobell DB (2019) Water use efficiency as a constraint and target for improving the resilience and productivity of C_3 and C_4 Crops. Annu Rev Plant Biol 70(1):781–808. doi:https://doi.org/10.1146/annurev-arplant-042817-040305

LeBauer DS, Treseder KK (2008) Nitrogen limitation of net primary productivity in terrestrial ecosystems is globally distributed. Ecology 89(2):371–379. doi:https://doi.org/10.1890/06-2057.1

Lefcheck JS (2016) PiecewiseSEM: Piecewise structural equation modelling in R for ecology, evolution, and systematics. Methods Ecol Evol 7(5):573–579. doi:https://doi.org/10.1111/2041-210X.12512

Leonardi S, Gentilesca T, Guerrieri R, Ripullone F, Magnani F, Mencuccini M, Noije TV, Borghetti M (2012) Assessing the effects of nitrogen deposition and climate on carbon isotope discrimination and intrinsic water-use efficiency of angiosperm and conifer trees under rising CO_2 conditions. Glob Change Biol 18(9):2925–2944. doi:https://doi.org/10.1111/j.1365-2486.2012.02757.x

Li J, Meng B, Chai H, Yang X, Song W, Li S, Lu A, Zhang T, Sun W (2019) Arbuscular mycorrhizal fungi alleviate drought stress in C_3 (*Leymus chinensis*) and C_4 (*Hemarthria altissima*) grasses via altering antioxidant enzyme activities and photosynthesis. Front Plant Sci 10:499. doi:https://doi.org/10.3389/fpls.2019.00499

Liang X, Zhang T, Lu X, Ellsworth DS, BassiriRad H, You C, Wang D, He P, Deng Q, Liu H, Mo J, Ye Q (2020) Global response

patterns of plant photosynthesis to nitrogen addition: A meta-analysis. Glob Change Biol 26(6):3585–3600. doi:https://doi.org/10.1111/gcb.15071

Mao Q, Lu X, Mo H, Gundersen P, Mo J (2018) Effects of simulated N deposition on foliar nutrient status, N metabolism and photosynthetic capacity of three dominant understory plant species in a mature tropical forest. Sci Total Environ 610:555–562. doi:https://doi.org/10.1016/j.scitotenv.2017.08.087

McAusland L, Vialet-Chabrand S, Davey P, Baker NR, Brendel O, Lawson T (2016) Effects of kinetics of light-induced stomatal responses on photosynthesis and water-use efficiency. New Phytol 211(4):1209–1220. doi:https://doi.org/10.1111/nph.14000

Meng B, Li J, Maurer GE, Zhong S, Yao Y, Yang X, Collins SL, Sun W (2021) Nitrogen addition amplifies the non-linear drought response of grassland productivity to extended growing-season droughts. Ecology 102(11):e03483. doi:https://doi.org/10.1002/ecy.3483

Niu S, Xing X, Zhang Z, Xia J, Zhou X, Song B, Li L, Wan S (2011) Water-use efficiency in response to climate change: from leaf to ecosystem in a temperate steppe. Glob Change Biol 17(2):1073–1082. doi:https://doi.org/10.1111/j.1365-2486.2010.02280.x

Olsen SR, Cole CV, Watanabe FS, Dean LA (1954) Estimation of available phosphorus in soils by extraction with sodium bicarbonate. USDA Circular 939:1–19

O'Mara FP (2012) The role of grasslands in food security and climate change. Ann Botany 110(6):1263–1270. doi:https://doi.org/10.1093/aob/mcs209

Ostertag R, DiManno NM (2016) Detecting terrestrial nutrient limitation: a global meta-analysis of foliar nutrient concentrations after fertilization. Front Earth Sci 4:23. doi:https://doi.org/10.3389/feart.2016.00023

Peng Y, Li F, Zhou G, Fang K, Zhang D, Li C, Yang G, Wang G, Wang J, Yang Y (2017) Linkages of plant stoichiometry to ecosystem production and carbon fluxes with increasing nitrogen inputs in an alpine steppe. Glob Change Biol 23(12):5249–5259. doi:https://doi.org/10.1111/gcb.13789

R Development Core Team (2020) R: a language and environment for statistical computing. R Foundation for Statistical Computing, Vienna

Ruiz M, Aguiriano E, Carrillo JM (2008) Effects of N fertilization on yield for low-input production in Spanish wheat landraces (*Triticum turgidum* L. and *Triticum monococcum* L.). Plant Breeding 127(1):20–23. doi:https://doi.org/10.1111/j.1439-0523.2007.01406.x

Shi B, Wang Y, Meng B, Zhong S, Sun W (2018) Effects of nitrogen addition on the drought susceptibility of the *Leymus chinensis* meadow ecosystem vary with drought duration. Front Plant Sci 9:254. doi:https://doi.org/10.3389/fpls.2018.00254

Stevens CJ, Lind EM, Hautier Y, Harpole WS, Borer ET, Hobbie S, Seabloom EW, Ladwig L, Bakker JD, Chu C, Collins S, Davies KF, Firn J, Hillebrand H, La Pierre KJ, MacDougall A, Melbourne B, McCulley RL, Morgan J, Orrock JL, Prober SM, Risch AC, Schuetz M, Wragg PD (2015) Anthropogenic nitrogen deposition predicts local grassland primary production worldwide. Ecology 96(6):1459–1465. doi:https://doi.org/10.1890/14-1902.1

Tian D, Wang H, Sun J, Niu S (2016) Global evidence on nitrogen saturation of terrestrial ecosystem net primary productivity. Environ Res Lett 11(2):024012. doi:https://doi.org/10.1088/1748-9326/11/2/024012

Tilman D (1987) Secondary succession and the pattern of plant dominance along experimental nitrogen gradients. Ecol Monogr 57(3):189–214. doi:https://doi.org/10.2307/2937080

van der Sleen P, Zuidema PA, Pons TL (2017) Stable isotopes in tropical tree rings: theory, methods and applications. Funct Ecol 31(9):1674–1689. doi:https://doi.org/10.1111/1365-2435.12889

Wang L, Delgado-Baquerizo M, Wang D, Isbell F, Liu J, Feng C, Liu J, Zhong Z, Zhu H, Yuan X, Chang Q, Liu C (2019) Diversifying livestock promotes multidiversity and multifunctionality in managed grasslands. Proc Natl Acad Sci USA 116(13):6187–6192. doi:https://doi.org/10.1073/pnas.1807354116

Wang Y, Wang D, Shi B, Sun W (2020) Differential effects of grazing, water, and nitrogen addition on soil respiration and its components in a meadow steppe. Plant Soil 447(1–2):581–598. doi:https://doi.org/10.1007/s11104-019-04410-5

Xiao L, Liu G, Li P, Xue S (2017) Nitrogen addition has a stronger effect on stoichiometries of non-structural carbohydrates, nitrogen and phosphorus in Bothriochloa ischaemum than elevated CO_2. Plant Growth Regul 83(2):325–334. doi:https://doi.org/10.1007/s10725-017-0298-8

Yang J, Zhang S, Li Y, Bu K, Zhang Y, Chang L, Zhang YJCGS (2010) Dynamics of saline-alkali land and its ecological regionalization in western Songnen Plain, China. Chin Geogra Sci 20(2):159–166. doi:https://doi.org/10.1007/s11769-010-0159-0

Yang X, Henry HAL, Zhong S, Meng B, Wang C, Gao Y, Sun W (2020) Towards a mechanistic understanding of soil nitrogen availability responses to summer vs. winter drought in a semiarid grassland. Sci Total Environ 741:140272. doi:https://doi.org/10.1016/j.scitotenv.2020.140272

Yu G, Jia Y, He N, Zhu J, Chen Z, Wang Q, Piao S, Liu X, He H, Guo X, Wen Z, Li P, Ding G, Goulding K (2019) Stabilization of atmospheric nitrogen deposition in China over the past decade. Nat Geosci 12(6):424–429. doi:https://doi.org/10.1038/s41561-019-0352-4